Proceedings 10th NUMGE 2023
10th European Conference on Numerical Methods in Geotechnical Engineering
Zdravkovic L, Kontoe S, Taborda DMG, Tsiampousi A (eds)

https://doi.org/10.53243/NUMGE2023-264

Numerical study on the penetration behaviour of drag-embedded anchor

Y.S Kuo[1], C.M. Chi[2], Y.H. Tseng[3], W.S. Khor[1], S.C. Chang[4], B.X. Jin[1]

[1]*Department of Hydraulic and Ocean Engineering, National Cheng-Kung University, Tainan, Taiwan*
[2]*Department of Civil Engineering, Feng Chia University, Taichung, Taiwan*
[3]*Chao Dao Environment and Energy Ltd. Kaohsiung, Taiwan*
[4]*CECI Engineering Consultants, Taipei, Taiwan*

ABSTRACT: The Taiwanese Government plans to develop the floating wind turbines for Round 3 offshore wind tenders, including at least one demonstration project. The water depths of the offshore wind farms in Taichung City and Hsinchu County are less than 100 m. The seabed at the sites consists of interbedded noncohesive and cohesive soils. For these offshore wind farms with floating offshore wind turbines, the catenary mooring system with drag-embedded anchors (DEAs) could be an option in commercial development. This study establishes a Coupled Eulerian-Lagrangian method (CEL) finite element (FE) model to analyse the anchor trajectory and holding capacity in cohesive soil with considering the effect of fluke geometry and layered soils. The results show good agreement between the FE analysis and theoretical analysis. The movement directions of the drag anchors are affected by the layered soil conditions significantly.

Keywords: Taiwan offshore wind farm; floating wind turbine; drag anchor; anchor trajectory; holding capacity

1 INTRODUCTION

The Taiwanese government intends to build floating wind farms for Round 3 potential offshore wind tenders, with a maximum of two demonstration projects. The water depths for the offshore wind projects in Taichung City and Hsinchu County (Figure 1) are less than 100 m. The seabed at the sites is comprised of interbedded noncohesive and cohesive soils.

Floating wind turbines have recently emerged as a feasible alternative to traditional fixed foundations for offshore wind turbines. Due to the spatial variation in soil properties at the site, ensuring proper anchor designs for the foundation is crucial for maintaining the stability of the wind turbine.

High-capacity drag embedment anchors are relatively simple anchoring methods to retrieve and reinstall, requiring the least amount of installation effort. The drag embedment anchors are also highly efficient with anchoring forces exceeding 20 times their dry weight (O'Neill et al., 1999).

Installing an offshore foundation can be more challenging and problematic with layered soil profiles. Understanding a drag-embedded anchor drag trajectory and capacity in layered clay profiles is the goal of this work.

This study builds on the work of Zhao and Liu, 2014 and Dou and Yu, 2018 in developing a CEL finite element model of drag embedded anchor (DEA) in two-layer soil profiles with variations of shear strength investigated.

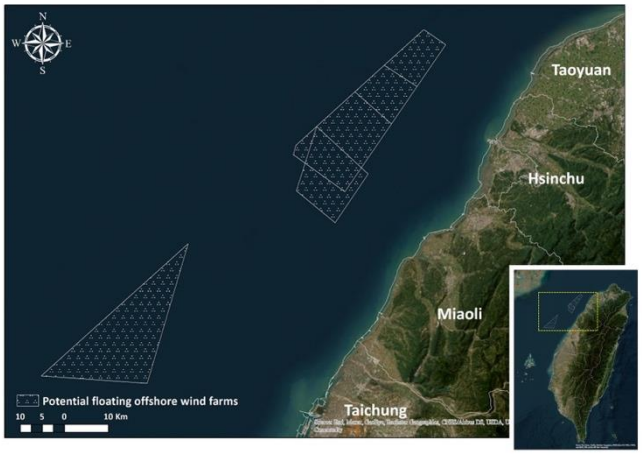

Figure 1. Potential floating wind farm in Taichung City and Hsinchu County

2 DEA TRAJECTORY PREDICTION METHODS

When investigating the issue of drag embedded anchors penetrating clayey soils, the empirical design charts provided by manufacturers have been used to predict the drag distance and holding capacity based on its dry weight and soil conditions. Considering the limitation of design charts, the mathematical approaches, including the limit equilibrium method and plastic limit analysis

method, are developed and simplified for analyzing the trajectory and capacity of anchors (Stewart 1992, Neubecker and Randolph, 1996), Dahlberg 1998, Ruinen 2004, Aubeny and Chi, 2010). Based on the results of theoretical analysis, the numerical models with coupled Eulerian-Lagrangian (CEL) method are established to simulate the large deformation behaviour of cohesive soil during the drag anchor installation phase (Zhao and Liu, 2014, Dou and Yu, 2018). Furthermore, for detailed soil profiles (layered soil), O'Neill et al., 1999 and Lai et al., 2020 conducted experimental methods and scaled the DEA model to obtain the behaviour of drag anchors in soils consisting of normally consolidated clay overlying silica sand and layered clay profiles respectively.

2.1 Limit equilibrium method

Neubecker and Randolph (1996) proposed the limit equilibrium analysis method based on the earlier study from Vivatrat et al. (1982), which presented the tangential and normal force equilibrium equations of a chain element (Figure 2) as Equations (1) and (2).

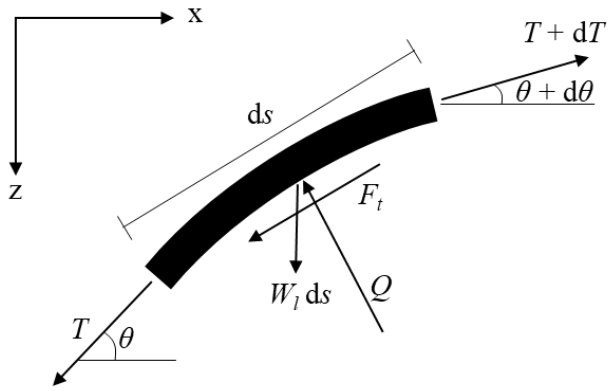

Figure 2. Force equilibrium of a chain element (redrawn from Neubecker and Randolph, 1996)

$$\frac{dT}{ds} = F_t + W_l \sin\theta \tag{1}$$

$$T\frac{d\theta}{ds} = -Q + W_l \cos\theta \tag{2}$$

where T is the tension in the chain, θ is the angle subtended by the chain to the horizontal, s is the distance measured along the chain starting at the attachment point, F_t and Q are the tangential and normal forces per unit length of the chain, respectively, and W_l is the buoyant weight of the chain per unit length.

In order to improve the effectiveness of iterative calculation, Neubecker and Randolph (1995) developed a simplified approach Equation (3), and for frictional development along the chain was derived as Equation (4), which results in a tension force T_0 at touch down point of the chain (Figure 3).

$$\frac{1}{2}T_a(\theta_a)^2 = z_a\bar{Q} \tag{3}$$

$$\frac{T_0}{T_a} = e^{\mu(\theta_a)} \tag{4}$$

where z_a is the depth of anchor. $\bar{Q}$ is the average bearing resistance (force per unit length) of the chain in the soil. θ_a is the attachment angle. μ is the friction coefficient between the chain and the soil.

Neubecker and Randolph (1996) expresses the penetration process of drag anchors in clayey soil with the assumption that the direction of anchor advancement is parallel to the fluke. the moment equilibrium considerations are used to calculate orientation changes of the anchor, taking into account the centers of pressure for each soil reaction. A new orientation of the anchor is also calculated by moment equilibrium considerations assuming centers of pressure for each of the soil reactions.

Figure 3 illustrates the force system of an embedded drag anchor in cohesive soil, where T_p is the geotechnical resisting force acting on the anchor parallel to the direction of movement (Equation (5)). Where f is the form factor for the anchor. A_p is the projected anchor area. N_c is the bearing capacity factor for the anchor line. S_u is the undrained shear strength of soil.

The combined force T_w of T_p and its normal component representing soil resistance can be calculated using Equation (6) with θ_w, which is taken as a constant. During the penetration process, θ_f is the angle between the fluke and the horizontal plane varies due to soil resistance, and its calculation is given by Equation (7).

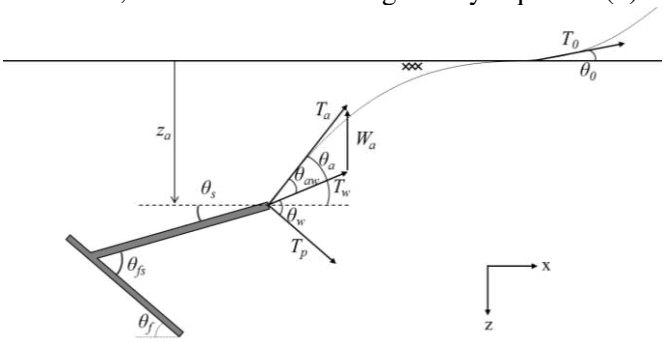

Figure 3. Anchor-chain system in cohesive soil

$$T_p = fA_pN_cs_u \tag{5}$$

$$T_w = \frac{T_p}{\cos\theta_w} \tag{6}$$

$$\theta_f = \theta_w + \theta_{aw} - \theta_a \tag{7}$$

3 NUMERICAL MODELING

This study follows Zhao and Liu (2014) and Dou and Yu (2018) to establish a Coupled Eulerian-Lagrangian method (CEL) finite element model with the software ABAQUS to analyse the anchor trajectory and holding capacity in cohesive soil.

3.1 Coupled Eulerian-Lagrangian (CEL) method

Figure 4 shows the geometry of the simplified anchor. Several solid cylinders simulate the anchor line with the LINK connector elements, which makes the distance of each cylinder constant. The length of the anchor line is 37.8 m, the cylinder length is 0.5 m, and the spacing is 0.1m. Anchor and anchor line is assumed as a Lagrangian rigid body. The soil model in this numerical model is simulated as elastic-perfectly plastic material with the Mohr-Coulomb failure criterion and discretized by Euler mesh.

A model is a symmetrical plane; only half of the anchor line and soil domain are analyzed in a 3D symmetrical FE model to reduce the computational cost, as shown in Figure 5. According to the ABAQUS User Manual (2020), Eulerian mesh element can pass through boundaries. It should be constrained by limiting the degrees of freedom of the nodes. As a result, the boundary conditions of the soil model can only be controlled through velocity conditions. The x-z plane of the soil model is configured with a y-direction velocity condition of 0. The x-direction velocity at y-z plane is set to 0. At the bottom of the soil model, the x-y plane also set the z direction velocity condition of 0. As for the anchor and chain model, the y-direction velocity condition is set to 0.

In the numerical model configuration, the anchor and anchor line model was laid flat on the seabed and dragged at the front end of the anchor line with a uniform speed. Liu and Zhao (2014) recommended that the drag velocity is one-quarter of the width of the fluke (w_f /4) in numerical analysis for DEA to ensure the simulation process is a quasi-static simulation.

The velocity of initial condition at drag point is 0m/s. the velocity of penetration is given a constant value v_d.Base on the suggestion in Liu and Zhao (2014), the value of v_d is w_f/4 s^{-1}, which keeps the model in Quasi-static Simulation.

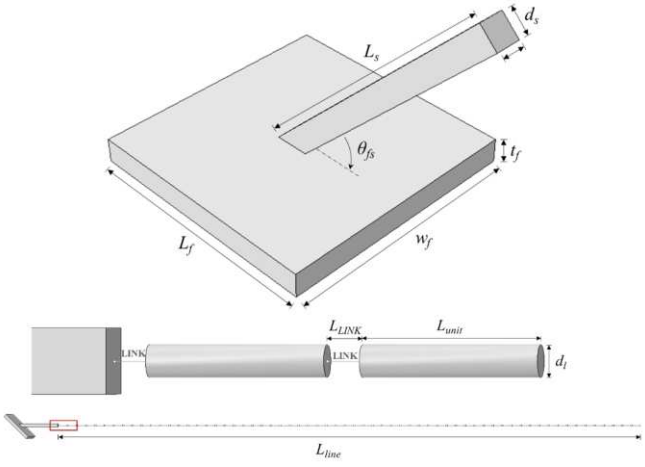

Figure 4. Anchor and anchor line model configuration

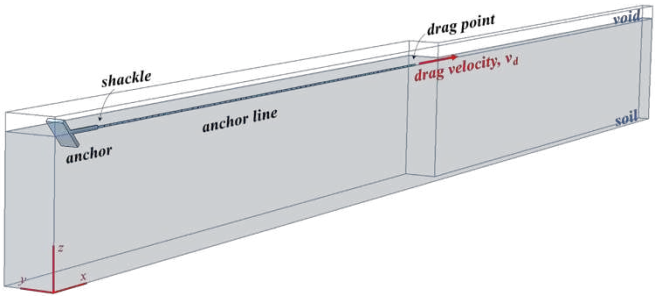

Figure 5. Soil model configuration

3.2 Model validation

The method for predicting the penetration trajectory and bearing capacity of DEA includes the empirical analysis method, theoretical analysis method, and numerical analysis. The holding capacity and trajectory of the numerical model in this study cooperated with the result obtained from the limit equilibrium analysis method, and the plastic limit analysis method in the theoretical method would be used to compare with the simulation result in this study.

The size of the rectangular fluke for model calibration is given in Table 1. The material parameters in the numerical model are given in Table 2.

Figure 6 shows the numerical simulation result of the anchors trajectory in the uniform clay soil. Comparing with the theoretically predicted trajectory of limit equilibrium method (Neubecker and Randolph, 1996), the analysis results show good agreement between both approaches.

Table 1. geometry of anchor and anchor line

Parameter		Value
Shank	Length, L_s	2.4 m
	Width, d_s	0.2 m
Rectangular fluke	Length, L_f	2 m
	Width, w_f	2 m
	Height, t_f	0.2 m
	Connected point, L_j	1 m
Fluke-shank angle, θ_{fs}		45°
Anchor line	Diameter, d_l	0.1 m
	Unit length, L_l	0.5 m
	Distance, L_{LINK}	0.1 m
	Length, L_{line}	37.8 m

Table 2.Material parameters of clay and steel

Material	Parameter	Value
Soft clay	Effective unit weight	7.5 kN/m^3
	Friction angle	0°
	Undrained shear strength	10 kPa
	Young's modulus	5000 kPa
	Poisson ratio	0.49
Steel	Effective unit weight	68 kN/m^3
	Young's modulus	2.1×10^8 kPa
	Poisson ratio	0.3

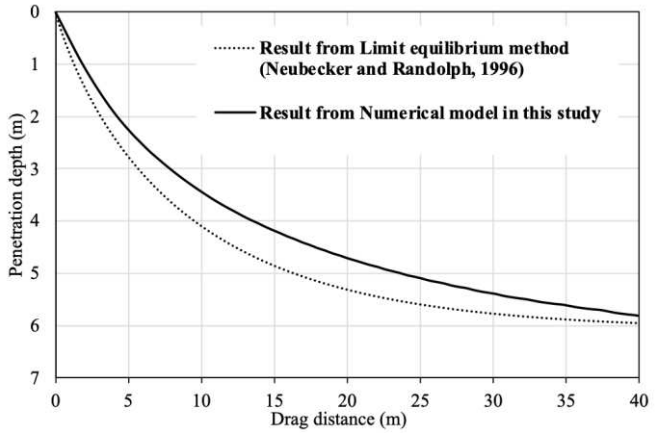

Figure 6. The trajectory prediction by numerical model and theoretical method

According to Figure 7, the trajectory of the anchor penetration is almost identical to the trajectories from the results from numerical methods of Zhao and Liu (2014) and Dou and Yu (2018).

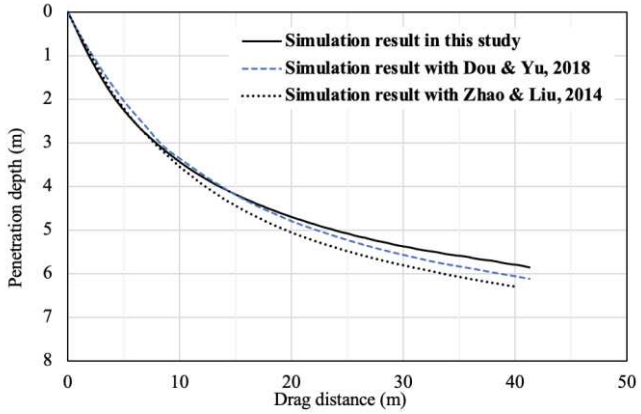

Figure 7. The trajectory prediction by numerical models

4 DEA TRAJECTORY PREDICTION IN LAYERED CLAYEY SOILS

To analyse the effect of the variation of soil strength on the penetration depth and holding capacity, this study expands the practical usefulness of the FE model for different soil conditions; the trajectory of DEA in a two-layered soil with the variation of shear strength is investigated, as listed in Table 3.

4.1 Model validation for layered soil

To investigate the effect of layered soil on embedded anchor penetration trajectory and anchor cable tension, an 8m-thick soil layer was established, with the first layer of soil depth ranging from 0 m to 4 m below the seabed surface and the second layer of soil depth ranging from 4 m to 8 m below the seabed surface (Case 1(b) in Table 3). To validate the 2-layered soil numerical model, the undrained shear strength of both layers is 10kPa; it is compared to the trajectory of single-layer soil (thickness = 8m) with the same soil strength S_u=10kPa (Case 1(a)).

It can be found in Figure 8 that when the drag distance reaches 40m, the penetration depth of the anchor into the layered soil is 5.7m, and the penetration depth of the anchor into the single layer of soil is 5.8m. The error between the two numerical models is only 2.7%, which shows that the numerical analysis model of embedded anchor penetration in layered soil could be applied to analyze the load-deformation reaction of the anchor in layered soils.

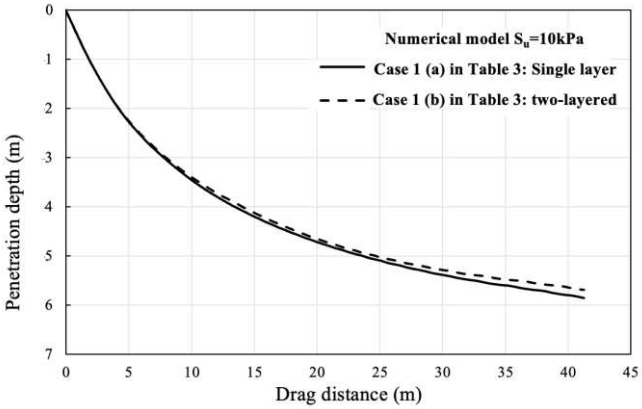

Figure 8. The trajectory prediction of single layer and 2-layered soil condition (Case 1 (a) and (b))

4.2 Numerical study on the penetration behaviour of DEA in layered clayey soils

A two-layered soil model is implemented in Case 2 and Case 3, incorporating two distinct undrained shear strengths S_u of the clay soil. In Case 2, the undrained shear strength S_u is 10kPa at the upper layer and 30kPa at the second layer. In Case 3, the undrained shear strength S_u of the first layer is 30 kPa and 10kPa in the second layer. The soil condition of three cases is listed in Table 3.

In Figure 9, when the Case 2 anchor horizontal drag distance reaches 13.5m, starts penetrating into the second layer, and its initial penetration path is identical with Case 1 (single layer soild). After dragging for a distance of 40m, the analysis of penetration depth reveals that Case 2 anchor is at the greatest depth, and Case 3 anchor is at the least depth.

As the Case 2 anchor enters from the softer soil layer to the harder soil layer, the drag anchor rotates and keys in the soil, making the penetration depth deeper at the same drag distance. On the contrary, when the anchor embeds from a harder soil layer to a softer soil layer (Case 3), the angle between the fluke and the horizontal plane θ_f become parallel to the interface of soil layers, and the penetration depth of the anchor is stagnant at about 4m as shown in Figure 10.

Comparing with the trajectories of 3 cases, when the anchor penetrates from the soft soil layer to the more complex soil layer, the position of the fluke adjusts with the penetration depth and continues to penetrate. However, when the anchor penetrates from the hard layer to the softer layer, the position of the fluke keeps

at a certain degree of intersection, and the anchor cannot be embedded smoothly in the soft layer below. In other words, if the hard soil layer overlying the softer soil layer, it may constrain the installation process of DEAs.

Table 3.soil condition of 3 cases

Case	depth	S_u (kPa)
1 (a) single layer	0~8m	10kPa
1 (b) Two-layered	0~4m	10kPa
	4m~8m	10kPa
2	0~4m	10kPa
	4m~8m	30kPa
3	0~4m	30kPa
	4m~8m	10kPa

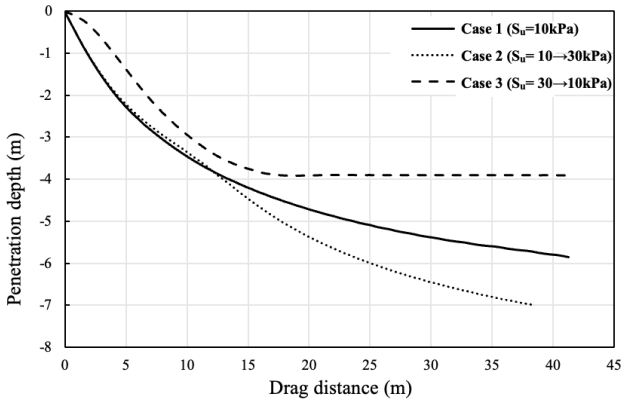

Figure 9. The trajectory prediction of 3 cases

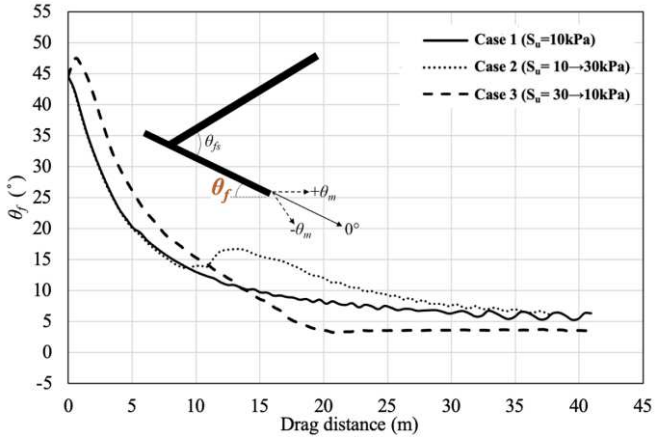

Figure 10. The angle between the fluke and the horizontal plane

4.3 Holding capacity of DEA in layered clayey soils

In the anchor installation process, the drag force at the shackle is usually regarded as the holding capacity. Therefore, when predicting the trajectory of the drag anchor with the plastic limit method, it is necessary to consider the response force of the anchor chain. Neubecker and Randolph (1995) proposed a theoretical solution by considering the anchor chain weight and small angle assumption. The drag force at the anchor T_a can be calculated with Equation (8).

$$T_a = \frac{2E_n N_c d S_u z}{\theta_a^2} \tag{8}$$

E_n is the multiplier to give the effective width in the expected direction; in this study, E_n =1, referring to Degenkamp and Dutta (1989). N_c is the bearing capacity factor for the anchor line, and N_c ranges from 9 to 14; this study uses 9 to calculate the T_a. d is the Diameter of anchor line. Finally, z is the depth of the anchor.

Figure 9 shows the holding capacity of DEA in different soil conditions. The deeper the anchor is embedded, the larger the holding capacity can be obtained.

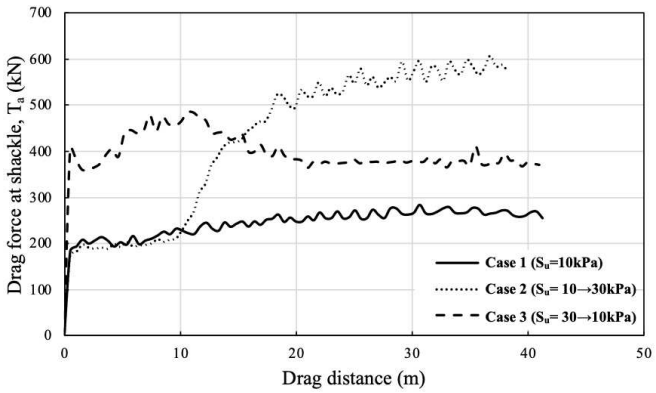

Figure 11. The holding capacity analysis of 3 cases

5 CONCLUSIONS

In this study, finite element software ABAQUS is used to establish a numerical model of drag embedded anchor and simulate its penetration behavior. To investigate the process of DEA penetration in soil, a finite element model validates with the results calculated with the equilibrium method and the numerical models from Zhao and Liu (2014) and Dou and Yu (2018). The results show good agreement between the FE analysis and theoretical analysis.

In addition, we extend the numerical model for calculating DEA trajectory and holding capacity in layered clayey soil. This study finds that when the anchor penetrates from a harder layer to a softer layer, the movement directions of the drag anchor could become a disadvantage of installation. The holding capacity increases when the DEA can be installed at a greater depth. This information can be used to select a location for DEA foundations to avoid unfavorable soil conditions.

6 ACKNOWLEDGEMENTS

This research was supported by the Ministry of Science and Technology of Taiwan and CECI Engineering Consultants, MOST 111-2622-E-006-028. The authors thank to National Center for High-performance Computing (NCHC) for providing computational and storage resources.

7 REFERENCES

Aubeny C. P., Chi C. 2010. Mechanics of drag embedment anchors in a soft seabed, *Journal of Geotechnical and Geoenvironmental Engineering*, 136(1): 57-68.

Dahlberg, R. 1998. Design procedures for deepwater anchors in clay, *Proc. of the 30th Annual Offshore Technology Conf.*, Houston, Texas.

Degenkamp, G., and Dutta, A. 1989. Soil resistances to embedded anchor chain in soft clay, *Journal of Geotechnical Engineering*, 115(10), 1420-1438.

Dou,Y.-Z. and Yu, L. 2018. Numerical investigations of the effects of different design angles on the motion behaviour of drag anchors, *Applied Ocean Research* 76, 199-210.

Lai, Y., Zhu, B., Huang, Y., and Chen, C. 2020. Behaviors of drag embedment anchor in layered clay profiles, *Applied Ocean Research* 101, 1.

Neubecker, S. R., Randolph, M. F. 1995. Profile and frictional capacity of embedded anchor chains, *Journal of geotechnical engineering*, 121(11), 797-803.

Neubecker, S. R., and Randolph, M. F. 1996. The performance of drag anchor and chain systems in cohesive soil, *Marine georesources and geotechnology*, 14(2), 77-96.

O'Neill, M.P., Randolph, M.F., House, A.R., 1999. The behaviour of drag anchors in layered soils. *International Journal of Offshore and Polar Engineering 9(1)*.

Ruinen, R.M., 2005. Influence of Anchor Geometry and Soil Properties on Numerical Modeling of Drag Anchor Behavior in Soft Clay. *Frontiers in Offshore Geotechnics ISFOG*.

Stewart, W.P., 1992. Drag Embedment Anchor Performance Prediction in Soft Soils. *Offshore Technology Conference*, Paper OTC 6970.

Vivatrat, V., Valent, P. J., & Ponterio, A. A. 1982. The influence of chain friction on anchor pile design, *Offshore Technology Conference*.

Zhao, Y. B., Liu, H. X. 2014. Numerical simulation of drag anchor installation by a large deformation finite element technique. *Proceedings of the ASME 2014 33rd International Conference on Ocean, Offshore and Arctic Engineering*.